Accepted Manuscript

T Cells Engineered to Express a T-cell Receptor Specific for Glypican Recognize and Kill Hepatoma Cells in Vitro and in Mice

Christina Dargel, Michal Bassani-Sternberg, Julia Hasreiter, Fabio Zani, Jan-Hendrik Bockmann, Frank Thiele, Felix Bohne, Karin Wisskirchen, Susanne Wilde, Martin F. Sprinzl, Dolores J. Schendel, Angela M. Krackhardt, Wolfgang Uckert, Dirk Wohlleber, Matthias Schiemann, Kerstin Stemmer, Mathias Heikenwälder, Dirk H. Busch, Günther Richter, Matthias Mann, Ulrike Protzer

PII: S0016-5085(15)00782-9
DOI: 10.1053/j.gastro.2015.05.055
Reference: YGAST 59826

To appear in: *Gastroenterology*
Accepted Date: 30 May 2015

Please cite this article as: Dargel C, Bassani-Sternberg M, Hasreiter J, Zani F, Bockmann J-H, Thiele F, Bohne F, Wisskirchen K, Wilde S, Sprinzl MF, Schendel DJ, Krackhardt AM, Uckert W, Wohlleber D, Schiemann M, Stemmer K, Heikenwälder M, Busch DH, Richter G, Mann M, Protzer U, T Cells Engineered to Express a T-cell Receptor Specific for Glypican Recognize and Kill Hepatoma Cells in Vitro and in Mice, *Gastroenterology* (2015), doi: 10.1053/j.gastro.2015.05.055.

T Cells Engineered to Express a T-cell Receptor Specific for Glypican Recognize and Kill Hepatoma Cells in Vitro and in Mice

Christina Dargel[1], Michal Bassani-Sternberg[2], Julia Hasreiter[1], Fabio Zani[3], Jan-Hendrik Bockmann[1,5], Frank Thiele[1,5], Felix Bohne[1], Karin Wisskirchen[1], Susanne Wilde[6], Martin F. Sprinzl[7], Dolores J. Schendel[6,9], Angela M. Krackhardt[9,10], Wolfgang Uckert[11], Dirk Wohlleber[12], Matthias Schiemann[8,9], Kerstin Stemmer[3], Mathias Heikenwälder[1], Dirk H. Busch[5,8,9], Günther Richter[4], Matthias Mann[2] and Ulrike Protzer[1,5,9]

[1] Institute of Virology, Technische Universität München / Helmholtz Zentrum München, Trogerstr. 30, 81675 München, Germany

[2] Max Planck Institute of Biochemistry, Am Klopferspitz 18, 82152 Martinsried, Germany

[3] Institute for Diabetes and Obesity, Helmholtz Zentrum München, Parkring 13, 85748 Garching, Germany

[4] Department of Pediatrics, University Hospital rechts der Isar, Technische Universität München

[5] German Center for Infection research (DZIF), Munich partner site

[6] Institute of Molecular Immunology, Helmholtz Zentrum München, Marchioninistraße 25, 81377 München, Germany

[7] I. Medizinische Klinik und Poliklinik, Universitätsmedizin der Johannes Gutenberg-Universität, Langenbeckstr. 1, 55131 Mainz, Germany

[8] Institute for Medical Microbiology, Immunology and Hygiene, Technische Universität München, Trogerstr. 30, 81675 München, Germany

[9] Clinical Cooperation Groups Antigen Specific Immunotherapy and Immune Monitoring, Technische Universität München / Helmholtz Zentrum München, Germany

[10] 3rd Medical Department, University Hospital rechts der Isar, Technische Universität München, Ismaninger Str. 22, 81675 München, Germany

[11] Max-Delbrück-Centrum for Molecular Medicine (MDC) and Institute of Biology, Humboldt University Berlin, Robert-Rössle-Straße 10, 13125 Berlin-Buch, Germany

[12] Institute of Molecular Immunology, University Hospital rechts der Isar, Technische Universität München, Ismaninger Str. 22, 81675 München, Germany

Corresponding Author: Prof. Ulrike Protzer, MD
Institute of Virology
Trogerstrasse 30, 81675 Munich, Germany
Phone: +49-89-4140-6821, Fax: +49-89-4140-6823
E-mail: protzer@tum.de

Short title: Glypican-3 T-cell therapy for hepatocellular carcinoma

Conflict of interest: Technische Universität München (with C.D. and U.P. as inventors) has filed a patent application for TCR P1-1 (EP14168107.2). The other authors have no conflict of interest to declare.

Grant support: The study was supported by the Helmholtz Allianz on Immunotherapy of Cancer (HAIT) HA-202 and by the German Research Foundation (DFG), SFB TR36 project A13, A14, T1, Z1; C.D. was supported by the Konrad-Adenauer-Stiftung, J.H.B. held a clinical leave stipend from the German Center of Infection Research.

Abbreviations: DC, dendritic cell; E:T, effector to target cell ratio; GPC3, glypican-3; HCC, hepatocellular carcinoma; HS, human serum; IFN, interferon; IL, interleukin; *ivt* RNA, *in vitro* RNA; moDC, monocyte derived DC; PBMC, peripheral blood mononuclear cells; SCID, severe combined immunodeficiency; SD standard deviation; TAA, tumor associated antigen; TCR, T-cell receptor; TRAV, TCR variable α-chain; TRBV, TCR variable β-chain; TIL, tumor-infiltrating lymphocytes; TNF, tumor necrosis factor

Author contributions: C.D. designed and performed research, analyzed data and drafted the manuscript. U.P. and M.F.S. designed the study, U.P. guided and supervised all experimental work and finalized the manuscript. M.B.S. performed mass spectrometry, corresponding data analysis and helped with manuscript preparation. M.H. performed immunohistochemistry. J.H., J.B., F.T., G.R. and F.Z. performed the *in vivo* experiments, K.S. and D.W. provided expertise and instrumentation. S.W., F.B., K.W., W.U., A.M.K. and D.J.S. supported T-cell receptor isolation and transfer. D.H.B. and M.S. prepared streptamers and provided cell sorting. All authors reviewed and edited the final manuscript.

Acknowledgements: We are grateful to Theresa Asen, Kathrin Kappes, Christina Neff, Natalie Röder, Kerstin Ackermann, Lynette Henkel and Petra Kotzbeck for excellent technical assistance. We thank Elisabeth Kremmer for providing antibodies, David Schirmer for providing mice and Richard Klar for sharing protocols. We also thank all blood donors.

Abstract

***Background & Aims*:** Cancer therapies are being developed based on our ability to direct T cells against tumor antigens. Glypican 3 (GPC3) is expressed by 75% of all hepatocellular carcinomas (HCC) but not in healthy liver tissue or other organs. We aimed to generate T cells with GPC3-specific receptors that recognize HCC and used them to eliminate GPC3-expressing xenograft tumors grown from human HCC cells in mice.

***Methods*:** We used mass spectrometry and to obtain a comprehensive peptidome from GPC3-expressing hepatoma cells after immune-affinity purification of HLA-A2, and used bioinformatics to identify immunodominant peptides. To circumvent GPC3-tolerance resulting from fetal expression, dendritic cells from HLA-A2 negative donors were co-transfected with GPC3 and HLA-A2 RNA to stimulate and expand antigen-specific T cells.

Results: Peptide $GPC3_{367}$ was identified as a predominant peptide on HLA-A2. We used A2-$GPC3_{367}$ multimers to detect, select for, and clone GPC3-specific T cells. These clones bound the A2-$GPC3_{367}$ multimer and secreted interferon-γ when cultured with $GPC3_{367}$, but not with control peptide loaded cells. By genomic sequencing of these T-cell clones, we identified a gene encoding a dominant T-cell receptor. The gene was cloned, the sequence was codon optimized and expressed from a retroviral vector. Primary $CD8^+$ T cells that expressed the transgenic T-cell receptor specifically bound $GPC3_{367}$ on HLA-A2. These T cells killed GPC3-expressing hepatoma cells in culture and slowed growth of HCC xenograft tumors in mice.

Conclusion: We identified a GPC3367-specific T-cell receptor. Expression of this receptor by T cells allows them to recognize and kill GPC3-positive hepatoma cells. This finding could be used to advance development of adoptive T-cell therapy for HCC.

Keywords: cancer immunotherapy; tumor-associated antigens; liver cancer; immune response

Introduction

Hepatocellular carcinoma (HCC) represents the second most frequent cause of cancer related death worldwide with approximately 800,000 cases per year.[1] In Africa and Asia, HCC has become the most common cause of cancer-related death due to the high prevalence of HBV and HCV infections. In Europe and in the USA, HCC incidence rapidly increases as a consequence of non-alcoholic steatohepatitis.[1] Its intrinsic resistance to chemo- and radiotherapy and the lack of effective treatment alternatives contribute to the poor outcome.[2] Thus, new therapeutic strategies are urgently needed.

Immune cell infiltration has been shown to be beneficial for patients with HCC. Prolonged patient survival has been reported to be associated with $CD8^+$ or NKT-cell infiltration.[3,4] These findings render immunotherapy and in particular adoptive T-cell therapy an interesting treatment strategy for HCC.

Allogeneic stem cell transplantation and last not least recent success with adoptive T-cell therapies utilizing *in vitro*-expanded, tumor-infiltrating lymphocytes and lately T-cell receptor (TCR) grafting have led to increasing enthusiasm in the field of cancer immunotherapy.[5] Grafting with TCRs that specifically recognize tumor-associated antigens (TAA) retargets patient's T cells towards tumor cells, and overcomes major drawbacks such as limited availability and low avidity of tumor-infiltrating lymphocytes.[6] A major limitation however is, that TAA usually are self-proteins expressed in fetal tissue and high avidity T cells recognizing TAA epitopes have been negatively selected during T-cell development in the thymus. Allorestricted T-cell stimulation, however, can circumvent this problem and allows isolation of high affinity TAA-specific TCRs.[7] We followed the idea that isolating high affinity TCRs against a typical TAA on HCC would pave the way for adoptive T-cell therapy as a new therapeutic approach.

HCC express a number of TAA that represent potential targets for antigen-specific adoptive T-cell therapy. Glypican-3 (GPC3), a 580 AA heparan sulphate proteoglycan, is expressed

during fetal development where it facilitates the interaction between growth factors and their receptors.[8] GPC3 is believed to play a role in the control of cell division and growth regulation, and its expression in HCC is associated with poor prognosis.[9] GPC3 is not expressed in healthy liver tissue but gets reactivated in ~75% of HCC, rendering GPC3 a suitable TAA for T-cell therapy even when its expression may show a mosaic pattern[10]. In the present study we stimulated GPC3-specific T cells in an allo-restricted fashion, isolated them by A2-GPC3 multimer staining and identified their specific TCR. Functionality and specificity of the isolated TCR towards human hepatoma cells was subsequently investigated *in vitro* and *in vivo*.

Materials and Methods

Stimulation of allo-restricted T cells. HLA-A2 RNA and GPC3 RNA were *in vitro* (*ivt*) transcribed and polyadenylated using the mMESSAGE mMACHINE T7 kit and Poly(A) tailing kit (both Life Technologies, Darmstadt, Germany). Mature monocyte-derived dendritic cells (moDC) were prepared from freshly isolated PBMC from a healthy HLA-A2 negative donor,[11] and maintained in low endotoxin RPMI1640 (Biochrom, Berlin, Germany) supplemented with 1.5% human serum and 50 IU/ml penicillin / streptomycin (P/S). MoDC were co-transfected with 35 µg GPC3 and 60 µg HLA-A2 *ivt*-RNA by exponential electroporation at 300 V and 150 µF (Gene Pulser Xcell, Bio-Rad, Munich, Germany). HLA-A2 and GPC3 expression was confirmed by flow cytometry after staining with α-GPC3-APC (R&D, Wiesbaden, Germany) and α-HLA-A2-FITC (BioLegend, London, UK) antibodies.

1×10^6 $CD8^+$ T cells (Dynabeads® Untouched™ Human CD8 T cells Kit, Life Technologies) were co-cultured with $1x10^5$ HLA-A2 and GPC3 *ivt*-RNA pulsed moDC from the same donor per well of a 24-well plate. 5 ng/ml IL-7 (PeproTech, Hamburg, Germany) were added on day 0 and 50 IU/ml IL-2 (Novartis, Quebec, Canada) on day 2 and thereafter every 3rd day. Primed T cells were restimulated at day 7 using freshly generated *ivt*-RNA pulsed moDC. T cells were maintained in human T-cell medium (hTCM): RPMI1640 dutch modified, 10% human serum (HS, isolated from healthy donors), 4 mM L-glutamine, 50 IU/ml P/S, 6 µg/ml

gentamycin, 1 mM sodium pyruvate and 1x non-essential amino acids (all from Life Technologies).

Multimer sorting and cloning of T cells. After 14 days of T-cell stimulation with moDC, HLA-A2 restricted GPC3-specific T cells were detected by staining with MHC-Streptamers (refolded A2-$GPC3_{367}$-streptag-fusion proteins multimerized with 0.4 µg PE-labelled Strep-Tactin (iba, Göttingen, Germany)) and α-CD8-APC (R&D).[12] A2-$GPC3_{367}$ multimer$^+$ $CD8^+$ T cells were enriched on a FACSAria^{TM} III cell sorter (BD Biosciences, Heidelberg, Germany) and cloned by limiting dilution in round-bottom 96-well plates containing $1x10^5$ irradiated (35 Gy) heterologous PBMC, $1x10^4$ irradiated (50 Gy) LCL-B27, 30 ng/ml α-CD3 (kindly provided by Elisabeth Kremmer, Helmholtz Zentrum München) and 50 IU/ml IL-2. After 14 days, GPC3-specific T-cell clones were identified by IFNγ ELISA (BioLegend) after co-incubation with peptide loaded T2 cells for 24 h. Specific T-cell clones were further expanded.

T-cell specificity. HLA-$A2^+$ and TAP deficient human lymphoma T2 cells[13], lymphoblastoid cell lines (LCL) expressing different HLA-A2 alleles, HLA-$A2^+$ $GPC3^+$ HepG2 or HLA-$A2^-$ $GPC3^+$ Huh7 cells were used as target cells. LCLs and T2 cells were maintained in hTCM without gentamycin. HepG2 and Huh7 cells were maintained in DMEM medium containing 10% FCS and otherwise the same supplements. T cells were co-incubated with $1x10^4$ peptide (iba) loaded (5 µM) target cells or $8x10^4$ human hepatoma cells in effector to target (E:T) ratios ranging from 0.2:1 to 5:1. After 24 h of co-culture supernatants were harvested and analysed by IFNγ ELISA.

TCR analysis and cloning of GPC3-specific TCRs. Total RNA was extracted from T-cell clones with Trizol and cDNA was synthesized using superscript III reverse transcriptase (both Life Technologies). TCR Vα- (TRAV) and Vβ-chains (TRBV) were PCR amplified using degenerated primers,[14] VPANHUM (TGAGTGTCCCPGAPGG2P) and CA2 (GTGACACATTTGTTTGAGAATC) for TRAV, VP1 (GCIITKTIYTGGTAYMGACA) or VP2

(CTITKTWTTGGTAYCIKCAG) and CP1 (GCACCTCCTTCCCATTCAC) for TRBV. TCR chains were identified by sequence analysis and blasting with IMGT/V-QUEST (Montpellier, France). Dominant TRAV and TRBV were optimized for mammalian codon usage and optimal gene expression (GeneOptimzer®), and according sequences were synthesized (GeneArt, Regensburg, Germany). TCR α- and β-chain were linked via a P2A element before the whole TCR construct was cloned into the retroviral vector pMP71[15] via *EcoRI* and *NotI* restriction sites. For improved pairing of the transgenic TCR, constant domains were murinized and an additional disulfide bridge was introduced.

Retroviral TCR transfer into human PBMC. Human embryonic kidney (HEK) 293T cells were co-transfected with 2 µg pMP71-TCR-P1-1, 1 µg pcDNA3.1-Mo-MLV and 1 µg pALF-10A1 using 10 µl lipofectamine (Life Technologies). In parallel freshly isolated human PBMC were activated on α-CD28 (eBioscience, Frankfurt, Germany) and α-CD3 coated 24-well plates in hTCM supplemented with 300 IU/ml IL-2. After 2 days, retrovirus was coated onto 24-well culture plates with 20 µg/ml RetroNectin (TaKaRa Bio Europe SAS, St. Germain en Laye, France) by centrifugation at 2000 g for 2 h. Cells were composed of approximately 20-30% activated $CD8^+$ and 50% $CD4^+$ T and 20-30% other cells at that stage. Subsequently $1x10^6$ activated T cells/well in hTCM supplemented with 100 IU/ml IL-2 were spinoculated at 1000 g for 10 min (all at 32 °C). A second transduc tion with fresh retrovirus was performed 24 h later. Transduction efficacy was analysed by A2-$GPC3_{367}$ multimer staining. Unless otherwise stated, PBMC transduced in the exactly same manner with a TCR recognizing the peptide 183-191 of hepatitis B virus S protein presented on HLA-A2 were used as mock control.

Functional assays. Transduced PBMC were analysed in IFNγ secretion assays as described above. Secretion of cytokines and translocation of LAMP-1 was furthermore investigated by intracellular cytokine staining with α-LAMP-1-PerCp-Cy5.5, α-IFNγ-FITC (eBioscience), α-IL-2-APC (BD Biosciences) and α-TNFα-PE (ImmunoTools, Friesoythe, Germany). To assess killing ability of transduced PBMC, the cells were co-incubated with

HLA-A2$^+$ GPC3$^+$ HepG2 or HLA-A2$^-$ GPC3$^+$ Huh7 cells that were seeded on 96-well E-plates (ACEA Biosciences, San Diego, USA). Target cell viability was acquired over time on an xCELLigence^{TM} SP (ACEA Biosciences) measuring viability via attachment strength of cells indicated by impedance measures.

Adoptive transfer of P1-1 expressing T cells *in vivo*. In a first experiment, 5x10^5 HepG2-luc cells were injected into the splenic pulp of 8 week-old female severe combined immunodeficiency (SCID)/Beige mice. In a second experiment, 3x10^6 cells were injected subcutaneously into the inguinal of 16- to 18-week old male recombinase activating gene-2 and common cytokine receptor gamma chain (Rag2$^{-/-}\gamma c^{-/-}$) double mutant mice. When tumors were established after 12 and 8 days, respectively, mice were injected intraperitoneally (i.p.) with 1x, 2x or 4x10^6 TCR$^+$ or mock transduced sorted CD8$^+$ human T cells in 200 µl PBS as indicated. Tumor growth was monitored by bioluminescence imaging using the IVIS Imaging system (PerkinElmer, Rodgau, Germany) every 3 to 7 days under anesthetizia with 2% isoflurane and 4 mg/kg coelenterazine (PJK, Kleinblittersdorf, Germany). For quantification, regions of interest (ROI) were selected and quantified as fold-increase in photons/second using Living Image Software (PerkinElmer).

Statistical analysis

Data is reported as mean values ± standard deviation (SD). To evaluate statistical differences between paired data sets the two-way-ANOVA with Bonferroni post-test was used. P values less than 0.05 were regarded as statistically significant. P values are indicated in the graphics as follows: $P>0.05$ (ns), $P<0.05$ (*), $P<0.01$ (**), $P<0.001$ (***). All analyses were performed with Prism 5.0 (GraphPad Software, Inc, La Jolla, USA).

Results

Identification of HLA-A2 restricted GPC3 peptides presented by human hepatoma cells.

Selecting the right epitope specificity is crucial for the development of effective T-cell therapies. It is therefore of utmost importance to choose epitopes that are presented at sufficient levels on the targeted tumor tissue. Using the bioinformatical prediction models SYFPEITHI[16], BIMAS[17] and NetMHC[18,19], 45 GPC3 peptides were predicted to bind the HLA-A2 molecules, among them 14 peptides were predicted by all three models (Table S1). To prioritize these peptides and identify which are presented after intracellular processing, we eluted peptides after immuno-affinity purification of HLA-I complexes from HLA-A2$^+$ GPC3$^+$ HepG2 cells[20] (Figure 1A). We identified in total 2004 unique HLA-I peptides (Table S2), most of which had a length of 9 amino acids (Figure 1B), among them the GPC3 peptides $GPC3_{367}$ (TIHDSIQYV) and $GPC3_{326}$ (FIDKKVLKV). Synthetic peptides were used to validate the mass spectrometry data (Figure S1). GPC3 epitopes are among the top 30% most abundant peptides, indicating a substantial presentation of these epitopes on the surface of HepG2 cells (Figure 1C). Because peptide $GPC3_{367}$ was predicted with higher affinity, we used this peptide for selection of TCRs.

Isolation of HLA-A2 restricted GPC3-specific T-cell clones.

Because GPC3 is expressed during fetogenesis[8] high-avidity GPC3-specific T cells have most likely undergone clonal deletion. To isolate high-avidity TCRs, we therefore employed an allo-restricted approach to stimulate GPC3-specific T cells (Figure 2A).

MoDC from an HLA-A2$^-$ donor were maturated[11] and transfected with ivtRNA to express HLA-A2 and GPC3. Surface expression of HLA-A2 was detected in 4% of moDC after 3 h and increased to stable surface expression in 56% of cells within 24 h, while GPC3 surface expression was detected in 24% of moDC after 3 h but not detectable anymore after 24 h (Figure 2B).

To expand GPC3-specific T cells, freshly generated HLA-A2 and GPC3 expressing moDC were used to stimulate $CD8^+$ enriched T cells from the same HLA-A2 negative donor. Antigen stimulation was repeated with newly prepared moDC after 7 days. On day 14 0.54% $CD8^+$ T cells bound the A2-$GPC3_{367}$ streptamer (Figure 2C) and were sorted for expansion of a GPC3-specific $CD8^+$ T-cell line. On day 21, the GPC3-specific T-cell line had been enriched to 57% double positive cells (Figure 2C), which was sorted again and immediately cloned by limiting dilution to obtain T-cell clones. Binding of A2-GPC3 $multimer^+$ (up to 98%) was confirmed in established T-cell clones (Figure 2C). Stimulation with untreated moDC served as background controls for all cloning stages (Figure S2).

To investigate functional specificity of our T-cell line and clones, we co-incubated them with peptide loaded T2 cells for 24 h. IFNγ was selectively secreted by the T-cell line and 19 out of 107 screened T-cell clones after co-culture with $GPC3_{367}$-loaded T2 cells but not with T2 cells loaded with an irrelevant peptide. Allo-reactive T-cell clones were identified by high IFNγ secretion levels on target cells loaded with both, $GPC3_{367}$ and irrelevant peptide. In Figure 2D, six representative GPC3-specific T-cell clones, one allo-reactive and one inactive clone are shown. Recognition of endogenously processed peptides by the T-cell line and by the selected T-cell clones was confirmed by recognition of $HLA\text{-}A2^+$ $GPC3^+$ HepG2 cells, while $HLA\text{-}A2^-$ $GPC3^+$ Huh7 cells used as control did not induce IFNγ secretion above background (Figure 2E).

Cloning and expression of $GPC3_{367}$-specific T-cell receptor P1-1.

The TCR repertoire of $GPC3_{367}$-specific HLA-A2 restricted T-cell clones was determined using degenerated primers for the amplification of TRAV and TRBV and subsequent sequencing. Sequence analysis revealed that one dominant TCR was expressed in all 19 selected $GPC3_{367}$-specific T-cell clones, referred to as P1-1 (Figure 3A). The identified TCR consisted of TRBV30*01 and TRAV8-3*02 (according to IMGT nomenclature). After correct pairing had been confirmed by co-expression, TRAV and TRBV sequences of the TCR were

codon-optimized to increase expression levels, and linked by a P2A element to ensure equimolar expression. For expression of TCR P1-1 in human T cells MLV-10A1 pseudotyped retroviral vectors were used. Surface expression of P1-1 before and after codon optimization was detected by staining with A2-$GPC3_{367}$ multimer on $CD8^+$ cells (Figure 3B). Characterization of transduced cells revealed that $CD4^+$, $CD8^+$ and $CD8^+CD56^+$ cells were transduced with P1-1 at comparable efficiency (Figure S3A). $CD8^+$ and $CD56^+CD8^+$ cells are referred to as $CD8^+$ T cells. Peptide-MHC specificity of P1-1 was confirmed using the irrelevant multimer A2-AFP_{325} (data not shown).

Peptide specificity and HLA-A2 dependency of TCR P1-1 grafted T cells.

To determine peptide specificity, we co-cultured P1-1 grafted T cells with peptide loaded T2 cells as target cells. Cells grafted with P1-1 secreted high levels of IFNγ after co-incubation only with $GPC3_{367}$ loaded T2 cells (Figure 4A). Because of T-cell stimulation via CD3/CD28 to enable retroviral transduction, basal IFNγ secretion was detected in all settings. To verify recognition of endogenously processed peptides, we assayed IFNγ secretion after co-culture with human hepatoma cells. IFNγ was secreted on HLA-$A2^+$ $GPC3^+$ HepG2 but not on Huh7 cells, which are $GPC3^+$ but HLA-$A2^-$. Finally, we analyzed IFNγ secretion after co-culture with human PBMC from HLA-$A2^+$ and HLA-$A2^-$ donors to exclude allo-recognition of HLA-A2 by P1-1 grafted cells (Figure 4A).

To determine the avidity of the TCR P1-1 we co-incubated P1-1 transduced T cells with T2 cells loaded with titrated $GPC3_{367}$ peptide concentrations. IFNγ secretion on target cells with irrelevant or without peptide equaled IFNγ secretion levels detected with mock transduced T cells and were set as background. Half maximal IFNγ secretion on peptide loaded T2 cells was observed with a peptide concentration of 100 nM (Figure 4B) corresponding to an intermediate functional avidity.

To evaluate the HLA-A2 allele dependency of TCR P1-1, we assessed P1-1 transduced T cells for their IFNγ secretion after co-incubation with peptide loaded LCL expressing different

HLA allotypes. This revealed that P1-1 recognizes $GPC3_{367}$ presented on HLA-A*02:01, 02:02, 02:07, 02:09, 02:16 and 02:17 (Figure 4C).

Effective killing of HLA-A2$^+$ GPC3$^+$ human hepatoma cells by TCR P1-1 grafted CD8$^+$ T cells.

To determine efficacy and kinetics of cytotoxicity achieved by TCR P1-1 grafting, we co-cultured TCR P1-1 transduced T cells at different E:T ratios with GPC3$^+$ HLA-A2$^+$ HepG2 cells and determined target cell viability over time. At an E:T ratio of 2.5:1 or 1.25:1 >95% of target cells were killed after 16 h (Figure 5A) with killing dynamics and efficiency showing a clear dose-dependency. Killing of target cells was still detected with E:T ratios as low as 0.15:1 after 6 days. Even at relatively high E:T ratios of 5:1, mock transduced T cells did not reduce viability of target cells (Figure 5A). Killing of HLA-A2$^-$ Huh7 and HepaRG hepatoma cells was only observed when HLA-A2 was reconstituted (Figure 5B,C).

Since not only CD8$^+$ T cells but also CD4$^+$ T cells can be transduced with TAA-specific TCR and may have beneficial function[21], we investigated expression and function of TCR P1-1 on CD8$^+$ vs CD4$^+$ T cells. Staining with the TRBV antibody showed that comparable proportions of CD8$^+$ and CD4$^+$ T cells (43 and 53%, repectively) expressed TCR P1-1 after transduction (Figure 6A). Although CD4$^+$ T cells were the dominant cell population, A2-$GPC3_{367}$ multimer binding was only detected in CD8$^+$ T cells (Figure 6A) indicating that stable peptide-MHC binding by P1-1 depends on additional binding of CD8 to the complex. To compare functionality of P1-1$^+$ CD8$^+$ and CD4$^+$ T cells, transduced cells were magnetically sorted for CD8$^+$ or CD4$^+$ cells and equal numbers of CD4$^+$ and CD8$^+$ T cells expressing P1-1 were co-incubated with HepG2 cells to analyze target cell viability over time. After co-culture with P1-1$^+$ CD8$^+$ T cells rapid killing of HepG2 cells was observed, while no difference between co-incubation with P1-1$^+$ CD4$^+$ T cells and T cells transduced with a mock TCR was detected (Figure 6B). When functionality was further assessed, CD8$^+$ (Figure 6C) but not CD4$^+$ T cells (Figure 6D) grafted with TCR P1-1 stained positive for intracellular IFNγ, IL-2 and TNFα and

mobilized LAMP-1 as a marker for degranulation on peptide $GPC3_{367}$ loaded T2 cells. Gating strategy for ICS is shown in Figure S3B. Sorted $CD8^+$ P1-1^+ T cells killed HepG2 cells faster than in the presence of $CD4^+$ T cells (Figure 6E) although after 12 h >90% killing was observed in both settings. Taken together, these results indicate that P1-1, which is of intermediate avidity, depends on binding of CD8 to increase binding affinity of the TCR complex.

Adoptive transfer of P1-1$^+$ T cells suppresses tumor growth in an in vivo HCC model.

To assess killing of $GPC3^+$ tumors by P1-1 grafted T cells *in vivo* we used a xenograft model, in which transplant tumors were established in immunodeficient mice using luciferase expressing HepG2-luc cells (Figure 7). In a first experiment, tumors were established in SCID/Beige for 12 days and then treated by adoptive transfer of TCR P1-1 or control TCR grafted human T cells. Tumor growth was efficiently suppressed by i.p. injection of $1x10^6$ P1-1^+ $CD8^+$ T cells (N=4) as compared to a control group receiving mock transduced cells (N=3) from the same healthy donor (Figure 7B, C). A tumor decrease was observed in 3 out of 4 animals treated with TCR P1-1 grafted T cells. Mouse #7 (Figure 7C, right panel) experienced a tumor relapse after initial response.

To confirm these results, we performed additional experiments using another mouse strain and a newly established cell line. Best results were obtained when mice where irradiated before T-cell transfer to improve engraftment (Figure 7D). As shown in Figure 7E, 21 $Rag2^{-/-}$ $\gamma c^{-/-}$ mice were transplanted by subcutaneous injection of $3x10^6$ HepG2-fluc cells s.c. into the inguinal. $2x10^6$ or $4x10^6$ P1-1^+ $CD8^+$ or mock-transduced T cells were injected after whole body irradiation and thereafter in weekly intervals. While P1-1 grafted T cells were initially able to control the tumor, they could only slow down tumor growth thereafter. This was accompanied by a lack of $CD8^+$ T cell infiltration into the tumor and by a reduced and mosaic-pattern GPC3 expression in comparison to cultured HepG2 cells (data not shown).

Discussion

The selection of immunogenic target antigens is the first crucial step for the development of an effective cancer immunotherapy. For this study we chose GPC3, because it is not expressed on healthy adult tissue but gets reactivated in about 75% of all HCC.[10] We identified two GPC3 peptides, $GPC3_{326}$ and $GPC3_{367}$, well presented on HLA-A2. We isolated T cells and out of these the TCR P1-1 recognizing the immunodominant peptide $GPC3_{367}$. Grafting primary $CD8^+$ T cells with TCR P1-1 rendered them polyfunctional effector cells. TCR P1-1 grafted T cells specifically recognized $GPC3_{367}$ on HLA-A2, effectively killed GPC3-positive cultured hepatoma cells and were even able to reduce established tumors *in vivo* in a murine transplantation model.

Using the prediction databases SYFPEITHI[16], BIMAS[17] and NetMHC[18,19], 45 GPC3 peptides were predicted to bind the HLA-A2 molecule. Using a mass spectroscopy analysis of the HLA-A2 peptidome, we only found two GPC3 peptides, $GPC3_{367}$ and $GPC3_{326}$ to be presented among the >2000 peptides isolated. This indicates, that proteasome cleavage, peptide loading and presentation of a TAA on MHC I is hard to predict[19]. On the other hand, it proves that GPC3 is a suitable TAA for T-cell targeting.

For selection of GPC3-specific TCRs, we decided to stimulate naive T cells in an allo-restricted fashion employing moDC expressing HLA-A2 and GPC3 after *ivt*-RNA transfection.[7] 16 $GPC3_{367}$-specific T-cell clones were identified that recognized HLA-$A2^+GPC3^+$ hepatoma cells and stained positive with an A2-$GPC3_{367}$ multimer. TCR analysis revealed a single TCR with identical CDR3 regions suggesting that all clones originated from the same T cell that had expanded. We codon-optimized variable and murinized constant TRAV and TRBV domains to increase expression and inter-chain affinity and reduce mispairing.[22] The optimized TCR P1-1 showed high surface expression and conferred effector function to $CD8^+$, but not to $CD4^+$ T cells proving dependency on additional binding of CD8 to the TCR-MHC complex. TCR P1-1 transduced T cells showed a rapid killing of HepG2 cells even with very low E:T ratios below 1:1 and recognized $GPC3_{367}$ in context of

HLA-A*02:01, 02:07 and 02:09 sharing identical peptide binding sites. $GPC3_{367}$ was also recognized in the context of HLA-A*02:02, 02:16 and 02:17, but not in the context of HLA-A*02:05, 02:06 and 02:08.

With half maximal secretion of IFNγ when target cells were loaded with 0.1 µM $GPC3_{367}$, functional avidity of TCR P1-1 was intermediate, which is in accordance with the functional avidity that has been observed for allo-restricted TCRs specific to other tumor antigens.[23] It is controversially discussed which functional avidity of TCRs is optimal for efficient anti-tumor immunotherapy, and whether or not high avidity goes along with better effector function and more efficient tumor eradication. T cells with high affinity TCRs show better functionality *in vitro*, but also more rapid exhaustion *in vivo*.[24,25] In addition, high T cell avidity can go along with substantial toxicity because rare cognate-antigen expressing cells may also be targeted.[26] Thus, an intermediate affinity may be advantageous.

Not only $CD8^+$, but also $CD4^+$ T cells can acquire cytotoxic capacities after adoptive transfer into patients.[27] In addition, $CD4^+$ T cells provide the necessary help for efficient $CD8^+$ T-cell function and to establish long-lived memory T-cell populations.[28] It has been shown that TCRs with high affinity can bind MHC I peptide complexes independent of CD8 co-expression, whereas MHC I peptide complex binding of lower affinity TCR depend on CD8 co-expression.[29] Our intermediate-affinity TCR P1-1 was CD8-dependent and was not able to activate $CD4^+$ cells, although we demonstrated expression on more than 50% of $CD4^+$ T cells by TRBV staining. The delayed killing of target cells in the presence of $CD4^+$ T cells that was observed might be interpreted as $CD8^+$ T-cell inhibition by regulatory T cells (T_{reg}), but could not detect enhanced expression of FoxP3 in CD4+ T cells after TCR P1-1 transduction (data not shown).

Specificity of TCRs is an important issue in T-cell therapy. TCR P1-1 equipped T cells specifically recognized peptide $GPC3_{367}$ in context of HLA-A2, while irrelevant peptides or $HLA\text{-}A2^+$ PBMC were not recognized. Thus, allo-reactivity of transduced T cells is very

unlikely. TCR P1-1 might be useful not only for adoptive T-cell therapy of HCC but also for patients with other GPC3-expressing tumors.[30] Squamous cell carcinoma of the lung, liposarcoma, melanoma and testicular nonseminomatous germ cell tumor were also found to express GPC3 in 50% of all analysed cases. For HCC, focal expression of GPC3 may limit efficacy, and GPC3 expression in non-HCC tissue such as dysplastic cirrhotic nodules may limit safety of adoptive T-cell therapy. In case of low-level expression, a TCR recognizing an MHC-peptide complex such as P1-1 maybe advantageous over an antibody[31] or chimeric antigen receptor[32] mediated therapy. Although it is encouraging that GPC3 directed antibody therapy proved safe in first clinical trials in HCC patients[31], GPC3 expression patterns may need to be studied in greater detail to avoid side effects of GPC3-specific TCR gene therapy.

T-cell therapy for solid tumors may finally have to be done as a combination approach. Since TAA-specific T cells in HCC often become exhausted[33], redirected T cells may be combined with checkpoint inhibitors to overcome immunomodulation by the liver microenvironment.[34] Since TAA often are not expressed at equal levels throughout an HCC but rather in a mosaic pattern, anti-GPC3 treatment may select GPC3-negative cells.[10] This most likely also occurred in our *in vivo* models. Using a combination of TCRs directed towards different TAAs would avoid selection of resistant cells. TCR P1-1 may be combined corresponding to the individual TAA expression profile of the tumor with TCRs specific for other TAA such as alpha-1-fetoprotein or NY-ESO-1. Since >50% of all HCC are induced by hepatitis B virus infection[2], combining virus-specific TCRs or chimeric antigen receptors[35,36] provides another alternative.

Results obtained in this study indicate that adoptive T-cell therapy is an interesting novel approach for the treatment of HCC and that GPC3 is a suitable target antigen. We describe two novel immunodominant HLA-A2-restricted epitopes in GPC3, identified TCR P1-1 that specifically recognizes peptide $GPC3_{367}$ and showed that this TCR confers T cell effector

function and allows efficient redirection of T cells against GPC3-positive HCC. This will help to pave the way for the development of adoptive T-cell therapy to fight HCC.

References

1. Forner A, Llovet JM, Bruix J. Hepatocellular carcinoma. Lancet 2012;379:1245-55.

2. Jemal A, Bray F, Center MM, et al. Global cancer statistics. CA Cancer J Clin 2011;61:69-90.

3. Chew V, Chen J, Lee D, et al. Chemokine-driven lymphocyte infiltration: an early intratumoural event determining long-term survival in resectable hepatocellular carcinoma. Gut 2012;61:427-38.

4. Gao Q, Qiu SJ, Fan J, et al. Intratumoral balance of regulatory and cytotoxic T cells is associated with prognosis of hepatocellular carcinoma after resection. J Clin Oncol 2007;25:2586-93.

5. Kershaw MH, Westwood JA, Darcy PK. Gene-engineered T cells for cancer therapy. Nat Rev Cancer 2013;13:525-41.

6. Marks DI, Lush R, Cavenagh J, et al. The toxicity and efficacy of donor lymphocyte infusions given after reduced-intensity conditioning allogeneic stem cell transplantation. Blood 2002;100:3108-14.

7. Wilde S, Geiger C, Milosevic S, et al. Generation of allo-restricted peptide-specific T cells using RNA-pulsed dendritic cells: A three phase experimental procedure. Oncoimmunology 2012;1:129-140.

8. Iglesias BV, Centeno G, Pascuccelli H, et al. Expression pattern of glypican-3 (GPC3) during human embryonic and fetal development. Histol Histopathol 2008;23:1333-40.

9. Shirakawa H, Suzuki H, Shimomura M, et al. Glypican-3 expression is correlated with poor prognosis in hepatocellular carcinoma. Cancer Sci 2009;100:1403-7.

10. Capurro M, Wanless IR, Sherman M, et al. Glypican-3: a novel serum and histochemical marker for hepatocellular carcinoma. Gastroenterology 2003;125:89-97.

11. **Dauer M, Obermaier B**, Herten J, et al. Mature dendritic cells derived from human monocytes within 48 hours: a novel strategy for dendritic cell differentiation from blood precursors. J Immunol 2003;170:4069-76.

12. Neudorfer J, Schmidt B, Huster KM, et al. Reversible HLA multimers (Streptamers) for the isolation of human cytotoxic T lymphocytes functionally active against tumor- and virus-derived antigens. J Immunol Methods 2007;320:119-31.

13. Salter RD, Howell DN, Cresswell P. Genes regulating HLA class I antigen expression in T-B lymphoblast hybrids. Immunogenetics 1985;21:235-46.

14. Zhou D, Srivastava R, Grummel V, et al. High throughput analysis of TCR-beta rearrangement and gene expression in single T cells. Lab Invest 2006;86:314-21.

15. Engels B, Cam H, Schuler T, et al. Retroviral vectors for high-level transgene

expression in T lymphocytes. Hum Gene Ther 2003;14:1155-68.

16. Rammensee H, Bachmann J, Emmerich NP, et al. SYFPEITHI: database for MHC ligands and peptide motifs. Immunogenetics 1999;50:213-9.

17. Parker KC, Bednarek MA, Coligan JE. Scheme for ranking potential HLA-A2 binding peptides based on independent binding of individual peptide side-chains. J Immunol 1994;152:163-75.

18. Nielsen M, Lundegaard C, Worning P, et al. Reliable prediction of T-cell epitopes using neural networks with novel sequence representations. Protein Sci 2003;12:1007-17.

19. Lundegaard C, Lamberth K, Harndahl M, et al. NetMHC-3.0: accurate web accessible predictions of human, mouse and monkey MHC class I affinities for peptides of length 8-11. Nucleic Acids Res 2008;36:W509-12.

20. Komori H, Nakatsura T, Senju S, et al. Identification of HLA-A2- or HLA-A24-restricted CTL epitopes possibly useful for glypican-3-specific immunotherapy of hepatocellular carcinoma. Clin Cancer Res 2006;12:2689-97.

21. Muranski P, Restifo NP. Adoptive immunotherapy of cancer using CD4(+) T cells. Curr Opin Immunol 2009;21:200-8.

22. Sommermeyer D, Uckert W. Minimal amino acid exchange in human TCR constant regions fosters improved function of TCR gene-modified T cells. J Immunol 2010;184:6223-31.

23. Felix NJ, Donermeyer DL, Horvath S, et al. Alloreactive T cells respond specifically to multiple distinct peptide-MHC complexes. Nat Immunol 2007;8:388-97.

24. Alexander-Miller MA, Leggatt GR, Berzofsky JA. Selective expansion of high- or low-avidity cytotoxic T lymphocytes and efficacy for adoptive immunotherapy. Proc Natl Acad Sci U S A 1996;93:4102-7.

25. Bendle GM, Holler A, Pang LK, et al. Induction of unresponsiveness limits tumor protection by adoptively transferred MDM2-specific cytotoxic T lymphocytes. Cancer Res 2004;64:8052-6.

26. Johnson LA, Morgan RA, Dudley ME, et al. Gene therapy with human and mouse T-cell receptors mediates cancer regression and targets normal tissues expressing cognate antigen. Blood 2009;114:535-46.

27. Hunder NN, Wallen H, Cao J, et al. Treatment of metastatic melanoma with autologous CD4+ T cells against NY-ESO-1. N Engl J Med 2008;358:2698-703.

28. Martin-Orozco N, Muranski P, Chung Y, et al. T helper 17 cells promote cytotoxic T cell activation in tumor immunity. Immunity 2009;31:787-98.

29. Johnson LA, Heemskerk B, Powell DJ, Jr., et al. Gene transfer of tumor-reactive TCR confers both high avidity and tumor reactivity to nonreactive peripheral blood mononuclear cells and tumor-infiltrating lymphocytes. J Immunol 2006;177:6548-59.

30. Baumhoer D, Tornillo L, Stadlmann S, et al. Glypican 3 expression in human nonneoplastic, preneoplastic, and neoplastic tissues: a tissue microarray analysis of 4,387 tissue samples. Am J Clin Pathol 2008;129:899-906.

31. Zhu AX, Gold PJ, El-Khoueiry AB, et al. First-in-man phase I study of GC33, a novel recombinant humanized antibody against glypican-3, in patients with advanced hepatocellular carcinoma. Clin Cancer Res 2013;19:920-8.

32. **Gao H, Li K**, Tu H, et al. Development of T cells redirected to glypican-3 for the treatment of hepatocellular carcinoma. Clin Cancer Res 2014;20:6418-28.

33. Gehring AJ, Ho ZZ, Tan AT, et al. Profile of tumor antigen-specific CD8 T cells in patients with hepatitis B virus-related hepatocellular carcinoma. Gastroenterology 2009;137:682-90.

34. Protzer U, Maini MK, Knolle PA. Living in the liver: hepatic infections. Nat Rev Immunol 2012;12:201-13.

35. Bohne F, Chmielewski M, Ebert G, et al. T cells redirected against hepatitis B virus surface proteins eliminate infected hepatocytes. Gastroenterology 2008;134:239-47.

36. **Krebs K, Bottinger N**, Huang LR, et al. T cells expressing a chimeric antigen receptor that binds hepatitis B virus envelope proteins control virus replication in mice. Gastroenterology 2013;145:456-65.

Author names in bold designate shared co-first authorship

Figure Legends

Figure 1. Identification of novel HLA-A2 restricted GPC3 peptides presented by human hepatoma cells.

(A) HLA-I complexes were immuno-affinity purified from HepG2 cells lysates using α-HLA-I (W6-32) antibody cross-linked to sepharose beads. HLA-I peptides were purified from the heavy chain based on their hydrophobicity. The enriched mixture of HLA-I peptides was measured on a quadrupole Orbitrap mass spectrometer (Q Exactive). Peptides sequences were identified using MaxQuant software. (B) Length distribution of 2004 HLA-I peptides identified from HepG2 cells shows the typical length of mainly 9-, 10- and 11-mer peptides. (C) Ranked measured intensity of the identified HLA-I peptides. Two epitopes from GPC3 proteins are among the top 30% supporting their high presentation level on surface of HepG2 cells.

Figure 2. Allo-restricted T-cell stimulation of GPC3-specific CD8$^+$ T cells with *ivt*-RNA pulsed dendritic cells.

(A) Schematic illustration of the allo-restricted stimulation protocol of naïve T cells with moDC pulsed with *ivt*-RNA. For details see Materials & Methods. (B) Expression of HLA-A2 and GPC3 after *ivt*-RNA transfection of DC was analysed 3 and 24 h post electroporation by flow cytometry. Gray curves represent mock-treated DC, black curves *ivt*-RNA transfected DC. Percentage of positive cells is indicated. (C) Bulk T-cell cultures (after two rounds of T-cell simulation with GPC3 and HLA-A2 *ivt*-RNA pulsed moDC), A2-GPC3$_{367}$ multimer enriched T-cell lines and T-cell clones established by limiting dilution cloning were stained with α-CD8 antibody and A2-GPC3$_{367}$ multimer and analyzed by flow cytometry. Percentage of A2-GPC3$_{367}^+$CD8$^+$ cells is indicated for each plot. (D) The A2-GPC3$_{367}$ multimer sorted T-cell line and derived T-cell clones were co-cultured with T2 cells loaded with 5 µM GPC3$_{367}$ or irrelevant peptide for 24 h at an E:T ratios of 0.2:1. IFNγ secretion was determined by ELISA. (C) Recognition of endogenously processed peptide was analyzed by co-culture with human hepatoma cells HepG2 (HLA-A2$^+$ GPC3$^+$) or Huh7 (HLA-A2$^-$ GPC3$^+$). Mean ± SD of triplicate co-cultures are given when sufficient numbers of T cells allowed experimental triplicates.

Figure 3. Cloning of TCR P1-1 and expression in CD8$^+$ T cells.

(A) TRAV and TRBV from functional GPC3$_{367}^+$ T-cell clones were amplified by PCR, codon-optimized and cloned into the retroviral vector pMP71 containing murinized constant TCR domains. PCR analysis of an exemplary clone is shown. TCR P1-1 with complete α- and β-chains linked by a P2A element is depicted schematically. (B) T cells transduced with TCR P1-1 before and after codon optimization transduced PBC were stained with anti-CD8 and A2-GPC3$_{367}$ multimer on day 4 post transduction and analyzed by flow cytometry. Percentage of CD8$^+$ GPC3$_{367}^+$ T cells detected is given.

Figure 4. Peptide specificity and HLA-A2 dependency of TCR P1-1 expressing T cells.

(A) TCR P1-1 and mock TCR transduced PBMC were co-cultured with T2 cells pulsed with 5 µM $GPC3_{367}$, irrelevant peptide (mock) or without peptide (w/o; left panel). IFNγ secretion after 24 h was measured by ELISA. In addition, transduced PBMC were co-cultured with HepG2 or Huh7 cells or PBMC from HLA-$A2^+$ or HLA-$A2^-$ donors (right panel). (B) T2 cells were loaded with $GPC3_{367}$ peptide at concentrations between 100 pM (10^{-10}) and 10 µM (10^{-5}) and used as target cells. (C) LCLs from different HLA-A2 subtypes were loaded with 5 µM $GPC3_{367}$ and used as targets for P1-1 or mock transduced PBMC. In all experiments, E:T ratios of 1:1 were used. Mean±SD of triplicate co-cultures are given.

Figure 5. Cytotoxicity of P1-1 grafted PBMC against human hepatoma cells.

(A) Cytotoxicity of TCR P1-1 expressing T cells was assayed by co-incubation with HepG2 cells at E:T ratios ranging from 0.15:1 to 2.5:1. (B) $GPC3^+$ but HLA-$A2^-$ HepaRG and (C) HuH7 cells were transduced with HLA-A2 and used as target cells at E:T ratios 1:1. Unspecific killing was investigated by comparison of HLA-$A2^-$ and HLA-$A2^+$ cells and by using mock-transduced PBMC as control. Viability of target cells was analyzed over time by impendence measurement using the xCELLigence™ system. Mean±SD of triplicate co-cultures are given at each time point.

Figure 6. Comparison of $CD8^+$ and $CD4^+$ TCR P1-1^+ grafted T cells.

(A) Expression of P1-1 in $CD8^+$ and $CD4^+$ T cells was investigated by flow cytometry following A2-$GPC3_{367}$ multimer staining and anti-TRBV staining. Percentages of cells staining positive are indicated. (B) Cytotoxicity was assayed by co-incubation of magnetically

sorted $CD8^+$ or $CD4^+$ T cells with HepG2 cells over time in comparison to mock-transduced PBMC. (C, D) Functionality of (C) $CD8^+$ and (D) $CD4^+$ T cells after co-incubation with $GPC3_{367}$ or mock peptide loaded T2 cells was examined. After 5 h of co-incubation, cells were harvested and intracellular cytokine and LAMP-1 staining were performed before analysis by flow cytometry. T cells transduced with mock TCR were used as control. (E) Cytotoxicity of TCR P1-1 expressing $CD8^+$ T cells and total PBMC was compared by co-incubation of P1-1^+ $CD8^+$ or P1-1^+ total PBMC with HepG2 cells. E:T ratios were 2:1. Viability of target cells was analyzed over time using the xCELLigence™ system. Mean ± SD of triplicate analyses are given.

Figure 7. Adoptive transfer of TCR P1-1^+ human T cells into a murine xenograft HCC model.

(A) Schematic overview: SCID/Beige mice were transplanted with HepG2-luc cells by intrasplenic injection. Based on the intensity of bioluminescence before treatment, mice received $1x10^7$ PBMC containing either $1x10^6$ TCR P1-1 or mock-transduced $CD8^+$ T cells i.p. (day 0). (B) Bioluminescence quantified 3 days before, at the day of T-cell transfer and 3 days thereafter is shown. Total luminescence was determined as total flux in photons / second in single mice and is plotted relative to initial measurement at day -3. (C) *In vivo* bioluminescence imaging of representative mice treated with TCR P1-1 grafted or mock grafted T cells is shown. Images were adjusted to the same pseudocolor scale to show relative bioluminescence changes over time. Color scale: min = 0 7.14e3; max = 0.35e5 photons. (D) Schematic overview: $Rag2^{-/-}\gamma c^{-/-}$ mice were transplanted with HepG2-fluc cells by s.c. injection, irradiated and received 2x or $4x10^6$ TCR P1-1 or $4x10^6$ mock-transduced $CD8^+$ T cells i.p. (transduction rate 50%) on day 0, 7 and 14. (E) Tumor growth was monitored by *in vivo* bioluminescence imaging. Fold-change of total flux per animal was

determined relative to day 0 at indicated time points. Mean values ± SEM (n=7 per group) are given.

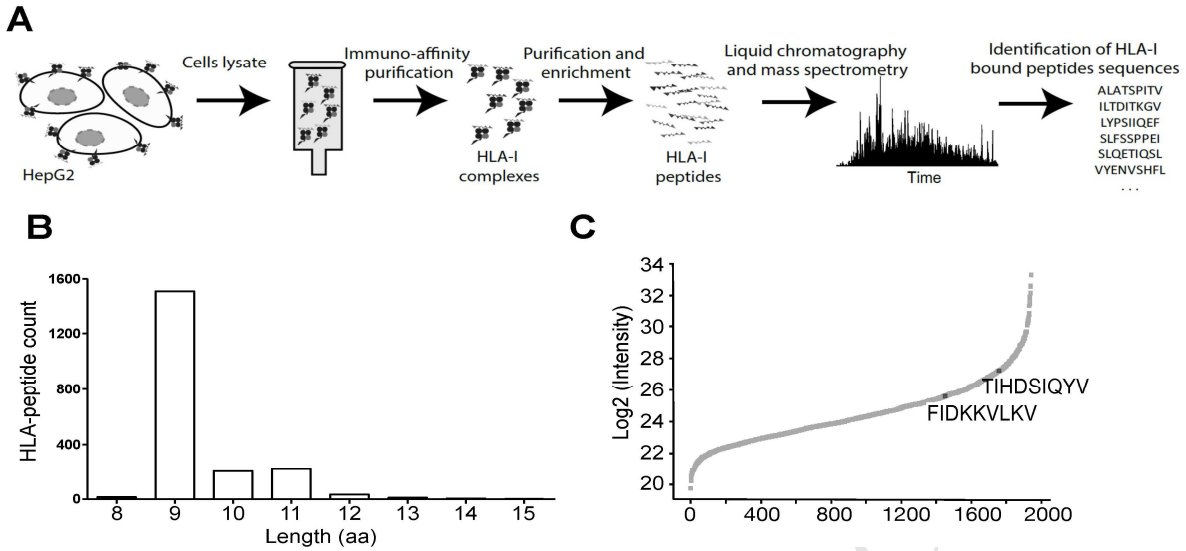

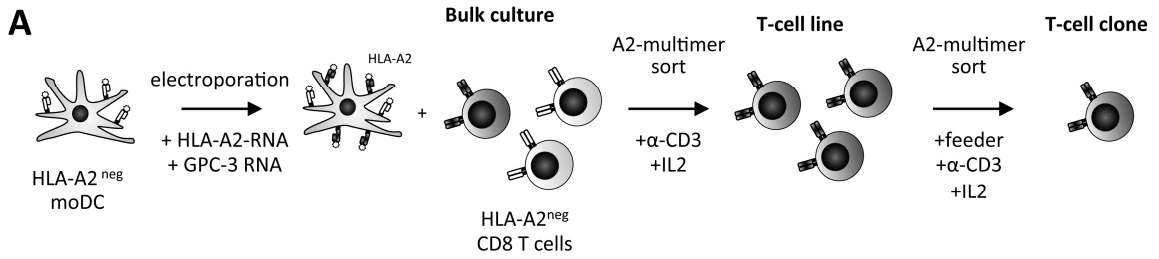
A
Bulk culture
T-cell line
T-cell clone
HLA-A2 neg
moDC
electroporation
+ HLA-A2-RNA
+ GPC-3 RNA
HLA-A2
HLA-A2neg
CD8 T cells
A2-multimer
sort
+α-CD3
+IL2
A2-multimer
sort
+feeder
+α-CD3
+IL2

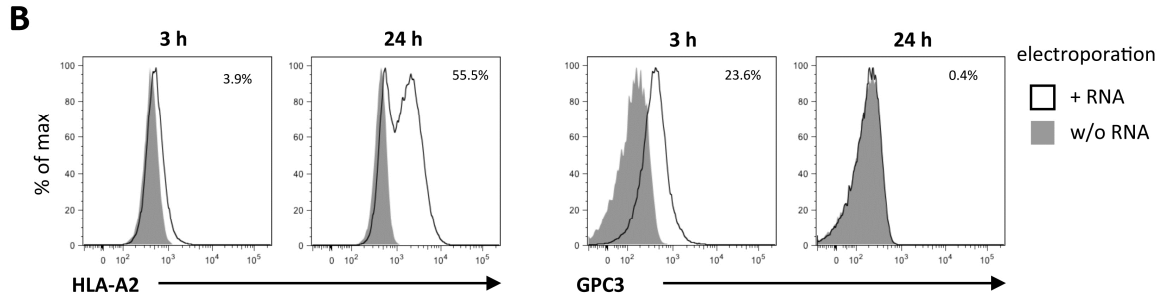
B
3 h
24 h
3 h
24 h
3.9%
55.5%
23.6%
0.4%
% of max
HLA-A2
GPC3
electroporation
+ RNA
w/o RNA

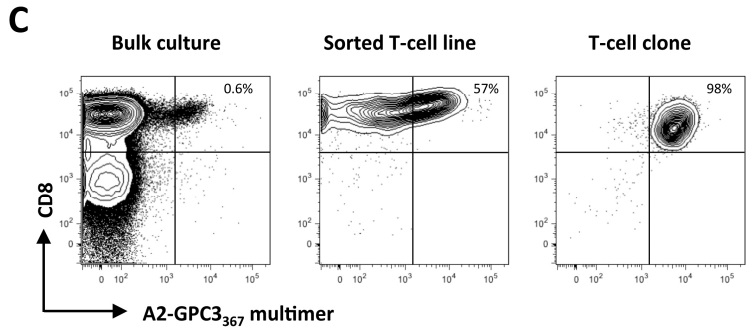
C
Bulk culture
Sorted T-cell line
T-cell clone
0.6%
57%
98%
CD8
A2-GPC3367 multimer

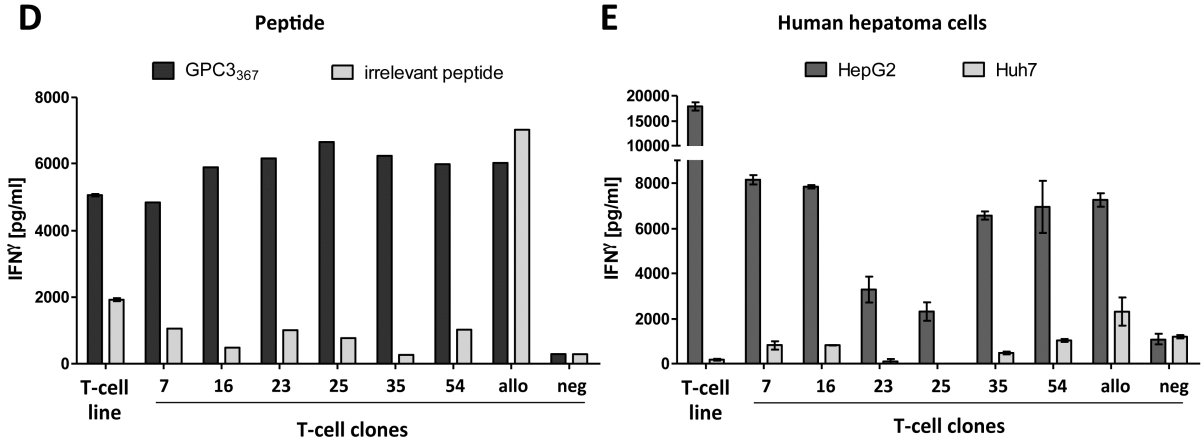
D
Peptide
GPC3367
irrelevant peptide
IFNγ [pg/ml]
T-cell line
7
16
23
25
35
54
allo
neg
T-cell clones
E
Human hepatoma cells
HepG2
Huh7
IFNγ [pg/ml]
T-cell line
7
16
23
25
35
54
allo
neg
T-cell clones

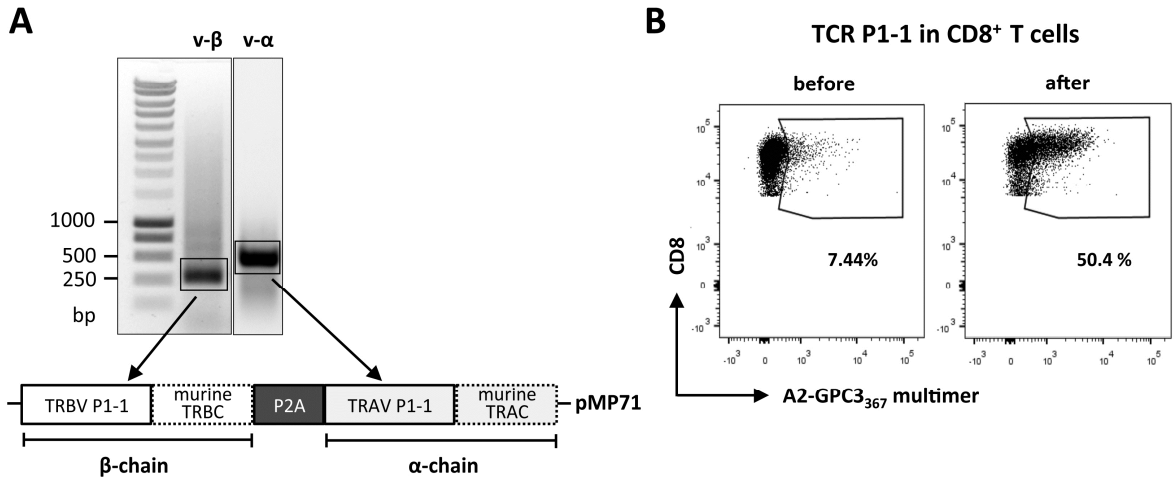

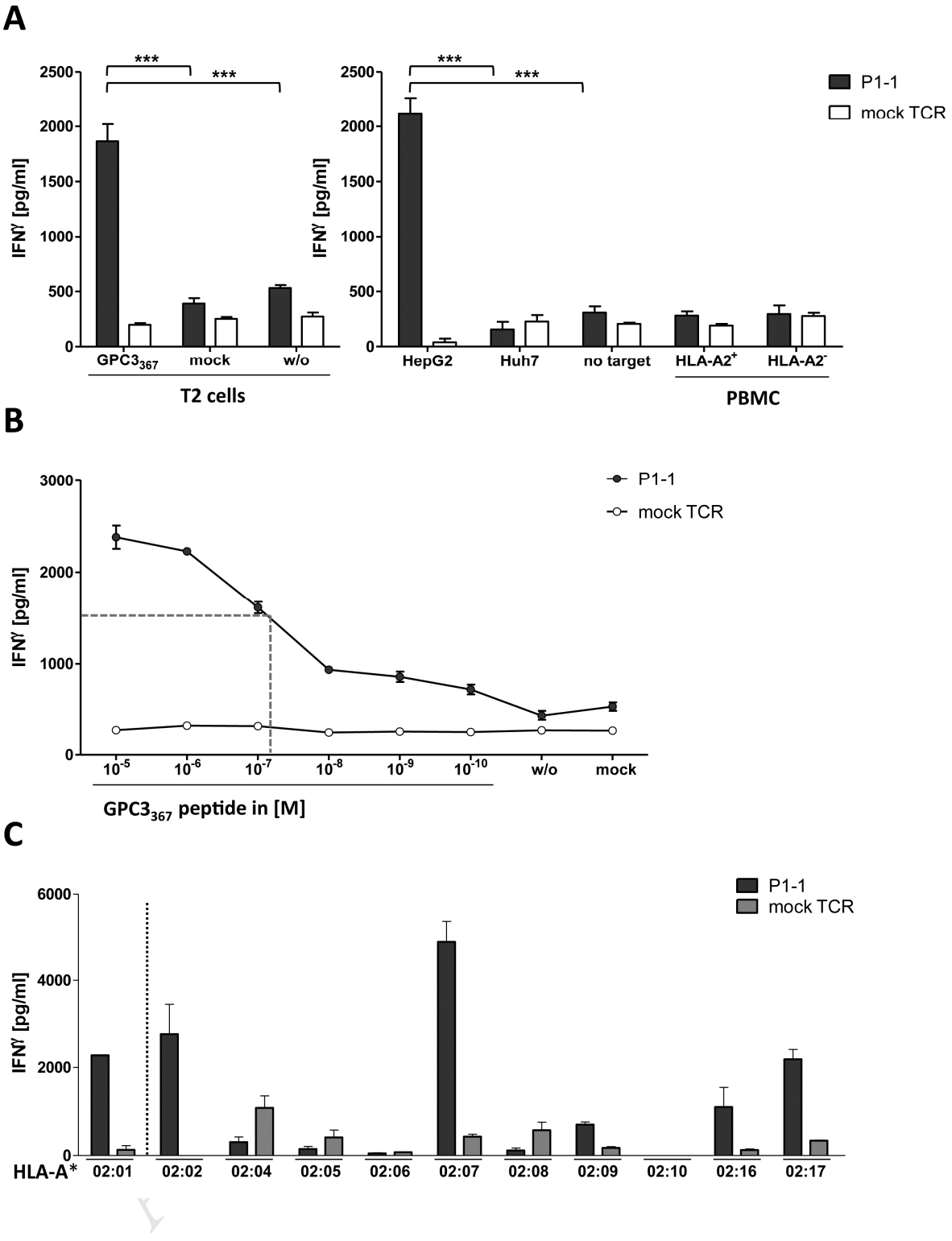
A
***
***
2500
2000
1500
1000
500
0
IFNγ [pg/ml]
GPC3367
mock
w/o
T2 cells
HepG2
Huh7
no target
HLA-A2+
HLA-A2-
PBMC
P1-1
mock TCR
B
3000
2000
1000
0
IFNγ [pg/ml]
10-5
10-6
10-7
10-8
10-9
10-10
w/o
mock
GPC3367 peptide in [M]
C
6000
4000
2000
0
IFNγ [pg/ml]
HLA-A*
02:01
02:02
02:04
02:05
02:06
02:07
02:08
02:09
02:10
02:16
02:17

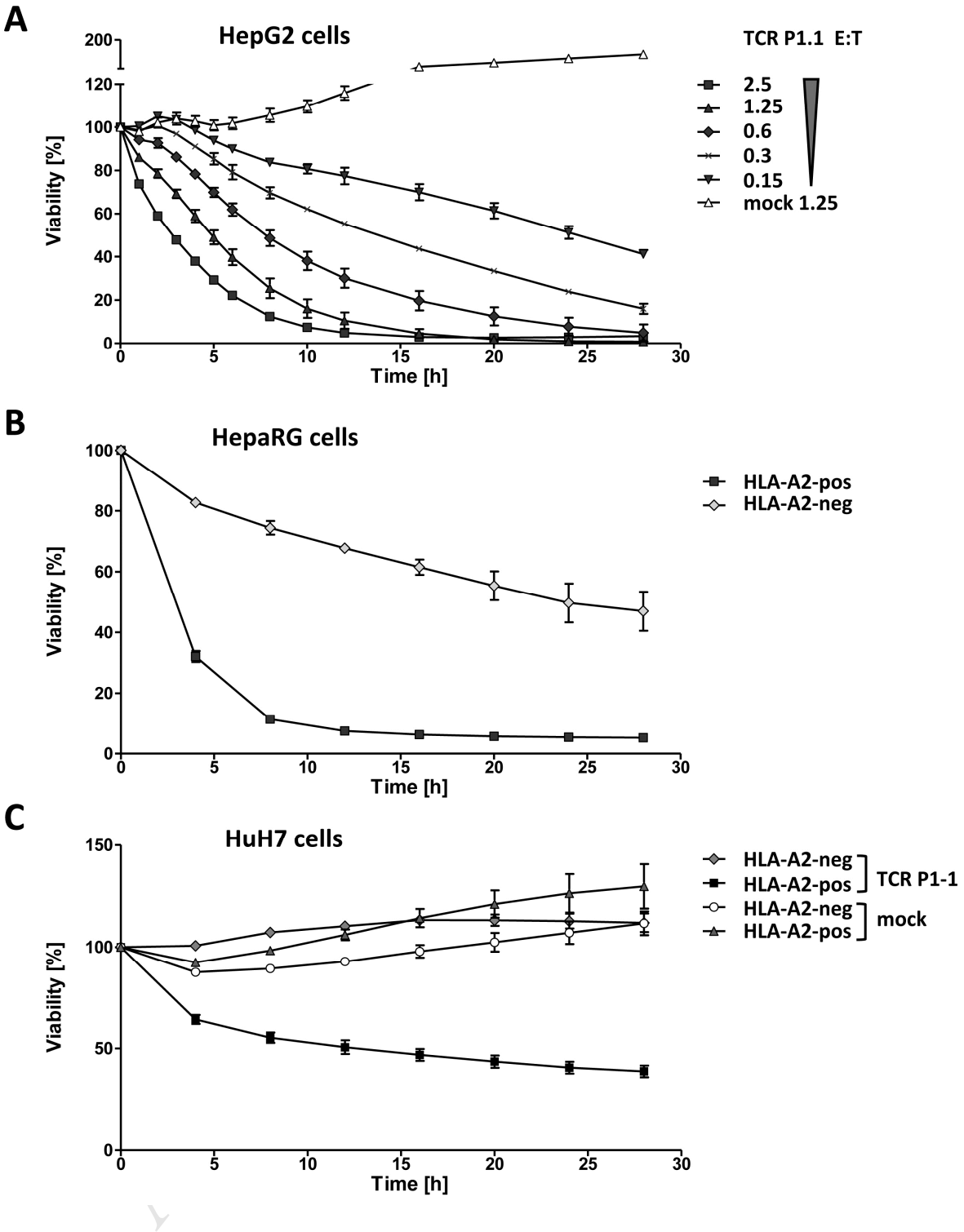
A
HepG2 cells
TCR P1.1 E:T
2.5
1.25
0.6
0.3
0.15
mock 1.25
Viability [%]
Time [h]
B
HepaRG cells
HLA-A2-pos
HLA-A2-neg
Viability [%]
Time [h]
C
HuH7 cells
HLA-A2-neg
HLA-A2-pos
TCR P1-1
HLA-A2-neg
HLA-A2-pos
mock
Viability [%]
Time [h]

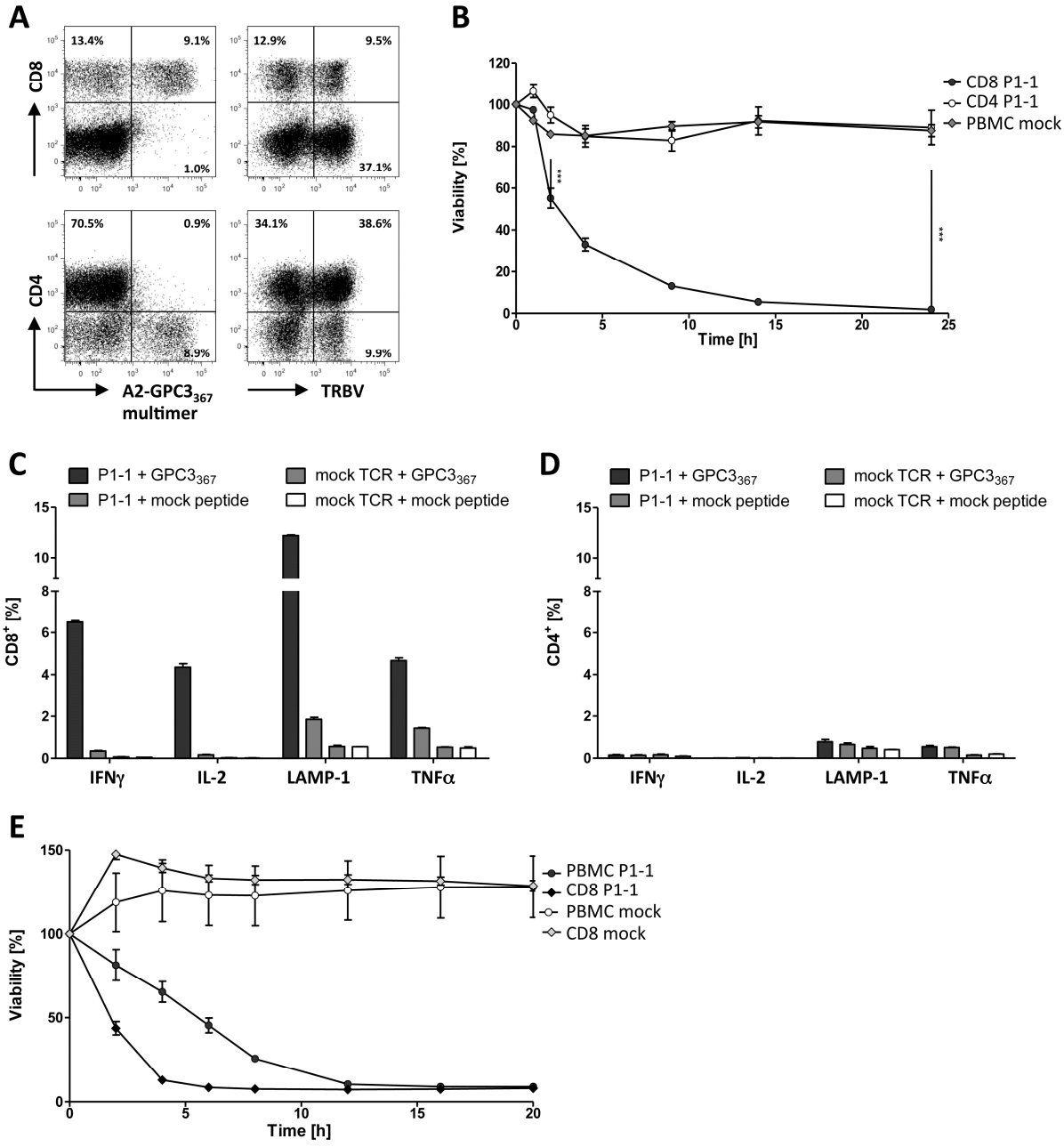
A
CD8
CD4
13.4%
9.1%
1.0%
12.9%
9.5%
37.1%
70.5%
0.9%
8.9%
34.1%
38.6%
9.9%
A2-GPC3367 multimer
TRBV
B
Viability [%]
Time [h]
CD8 P1-1
CD4 P1-1
PBMC mock
***
C
P1-1 + GPC3367
P1-1 + mock peptide
mock TCR + GPC3367
mock TCR + mock peptide
CD8+ [%]
IFNγ
IL-2
LAMP-1
TNFα
D
CD4+ [%]
E
Viability [%]
Time [h]
PBMC P1-1
CD8 P1-1
PBMC mock
CD8 mock

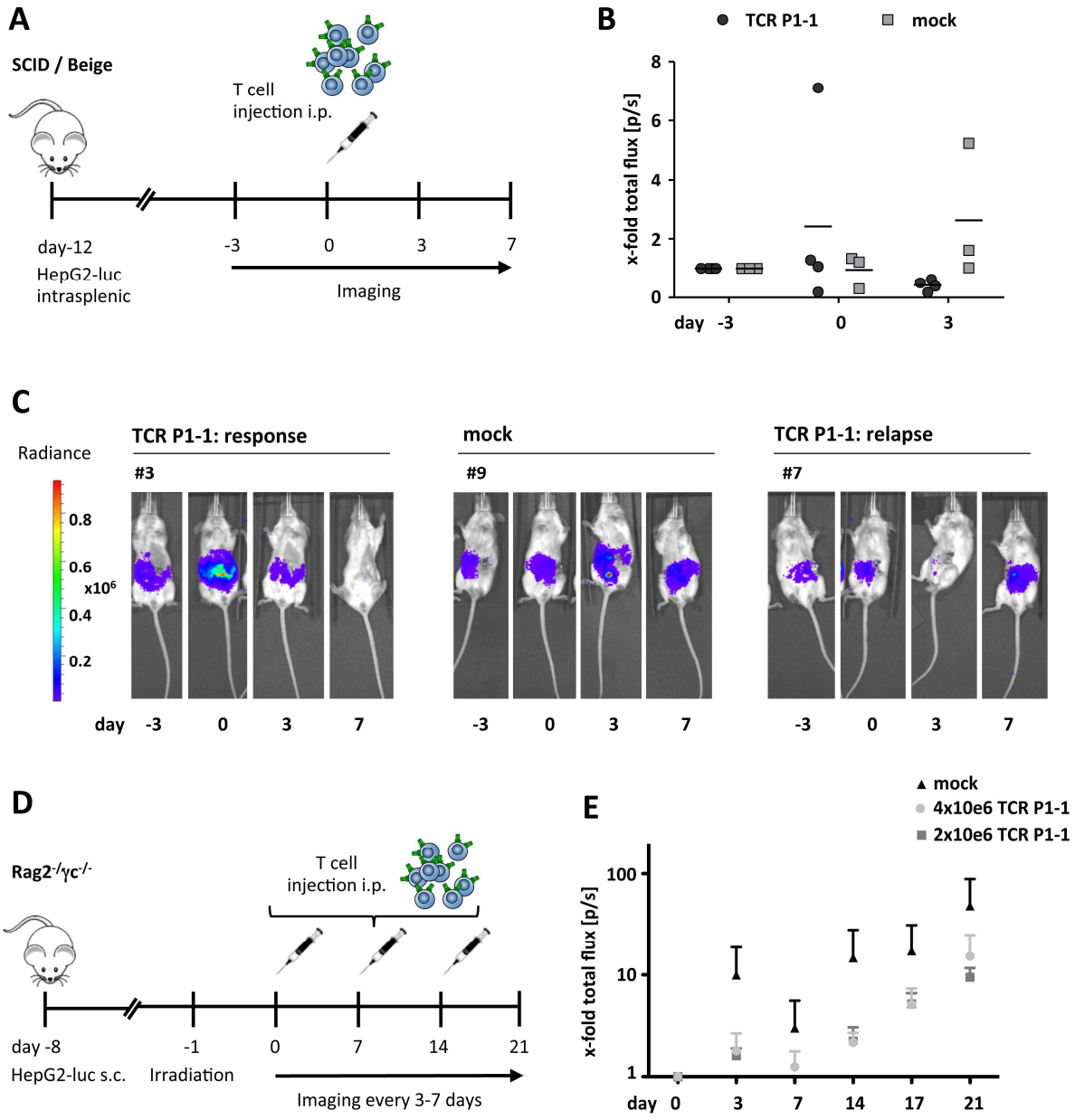

A

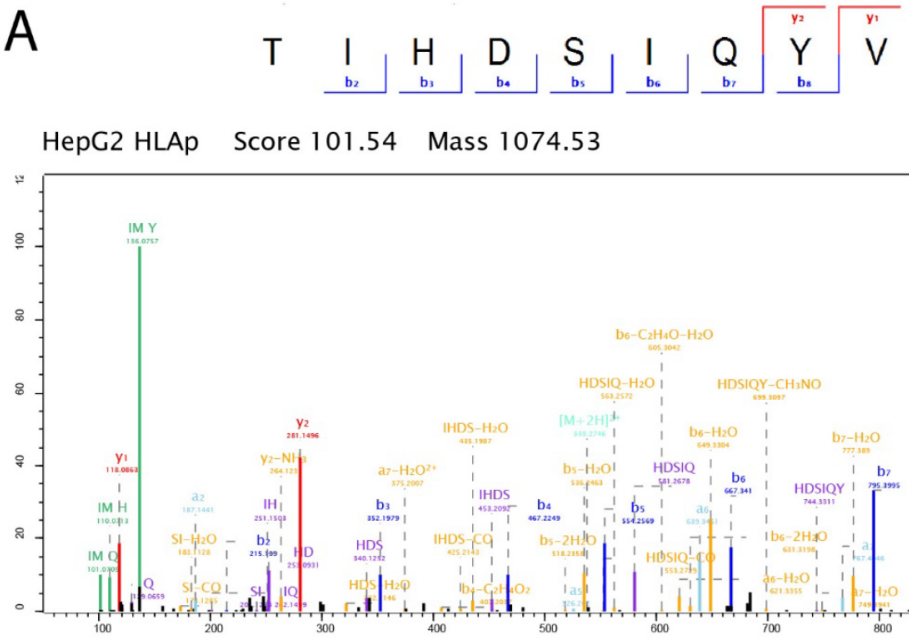

1

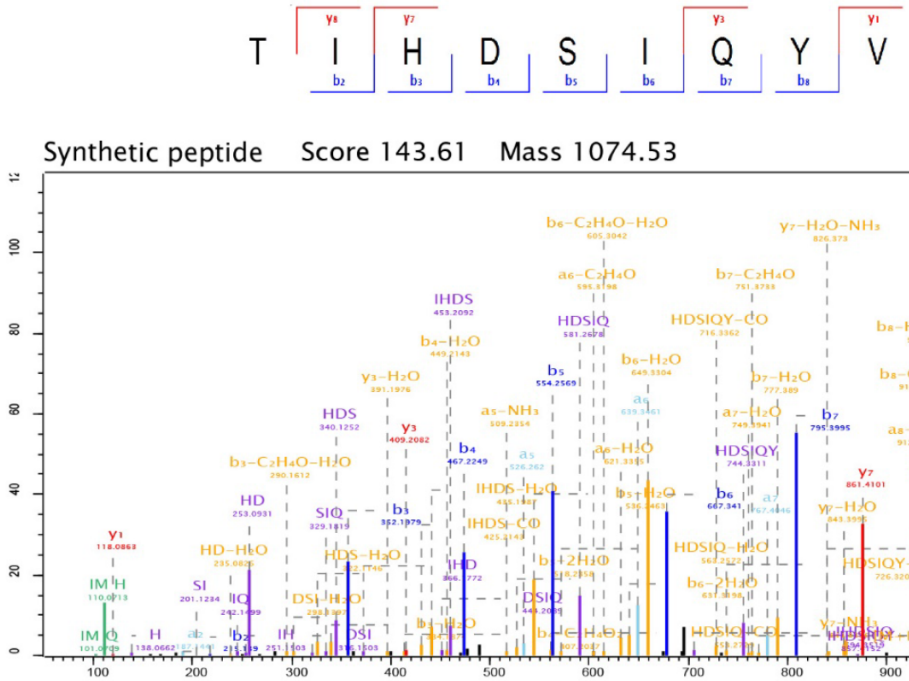

2

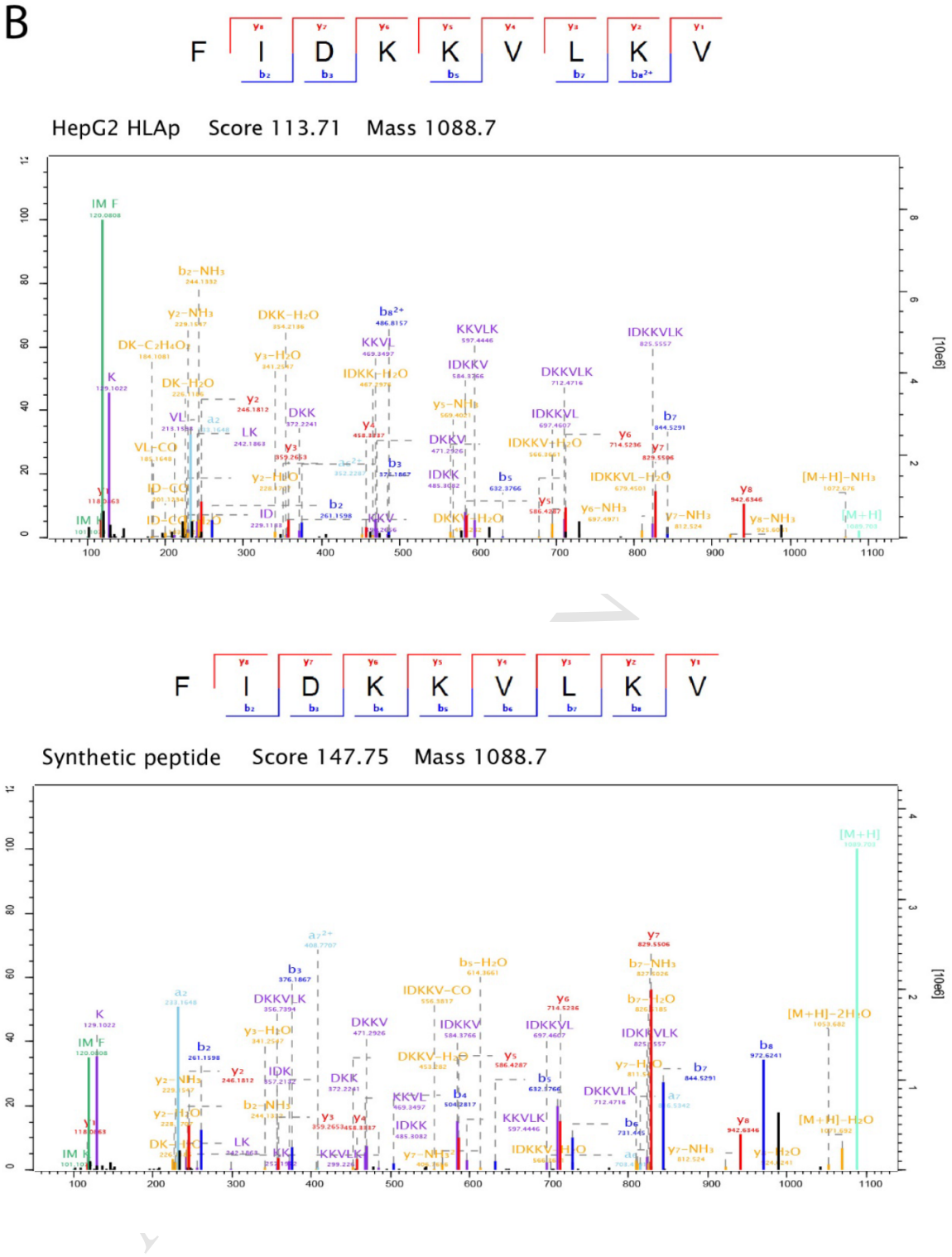

Figure S1: Mass spectrometry of peptides eluted from HLA-A2. Mass spectra of (A) $GPC3_{367}$ (TIHDSIQYV) and (B) $GPC3_{326}$ (FIDKKVLKV). Mass spectra of the two purified peptides and their synthetic counterparts are shown.

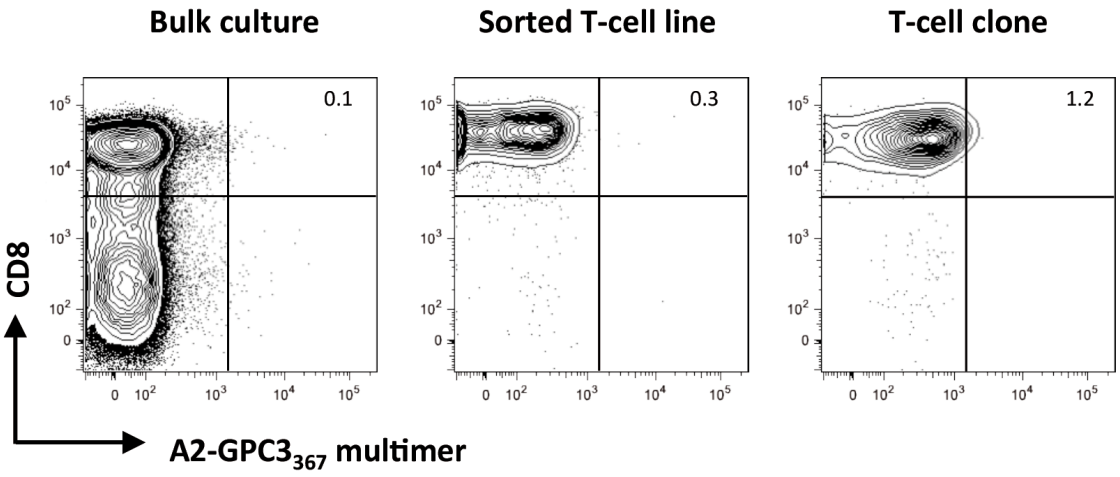

Figure S2: Negative control stimulation of T-cells. Bulk T-cell cultures after two cycles of T-cell simulation with untreated moDC, A2-GPC3$_{367}$ multimer enriched T-cell lines and T-cell clones established by limiting dilution cloning were stained with α-CD8 antibody and A2-GPC3$_{367}$ multimer for flow cytometry. Percentage of A2-GPC3$_{367}$ multimer^{+} CD8^{+} cells is shown in the upper right corner of each plot.

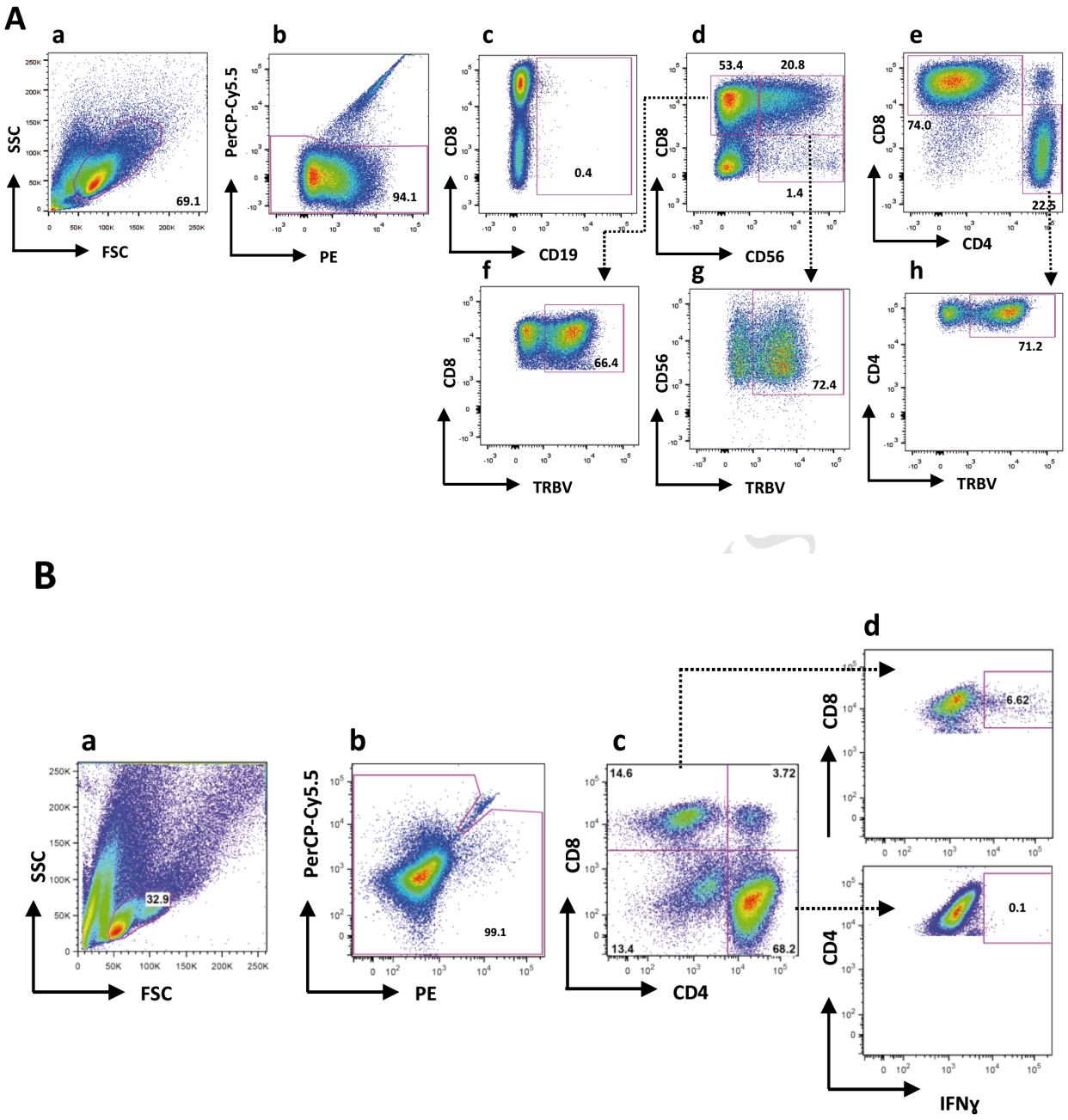

16 **Figure S3: Representative gating strategies for ICS. (A)** Lymphocytes were identified by
17 typical FSC/SSC parameters (a), discriminated from dead cells (b: Live Dead-) and then
18 analyzed for surface markers (c: CD8, CD19, d: CD8, CD56, e: CD8, CD4). Transduction
19 rate of $CD8^+$ $CD56^-$ (f), $CD8^+$ $CD56^+$ (g) and $CD4^+$ (h) cells was identified by TRBV
20 (percentage of positive cells is indicated). **(B)** Lymphocytes were identified by typical
21 FSC/SSC parameters (a), discriminated from dead cells (b: Live Dead-) and then analyzed
22 for surface markers (c: CD8, CD4). After ICS cytokine secreting $CD8^+$ or $CD4^+$ T cells were
23 identified (d: IFNɣ+).

Supplementary Methods

Affinity purification of HLA molecules. HLA-I complexes were purified from two biological replicates of $5x10^8$ HepG2 cells lysed with 0.25% sodium deoxycholate, 0.2 mM iodoacetamide, 1 mM EDTA, 1:200 Protease Inhibitors Cocktail (Sigma), 1 mM phenylmethanesulfonyl fluoride (Sigma), 1% octyl-β-D glucopyranoside (Sigma) in PBS at 4 °C for 1 h. The lysates were cleared by 30 min centrifugation at 40,000 g. HLA-I molecules from cleared lysate were immunoaffinity purified with the W6/32 antibody, which was purified from the growth medium of HB-95 hybridoma cells, covalently bound to protein-A Sepharose beads (Invitrogen, CA). The affinity column was thoroughly washed first with 10 column volumes of 150 mM NaCl, 400 mM NaCl and 150 nM NaCl containing and pure 20 mM Tris HCl, pH 8.0, each. HLA-I molecules were eluted at room temperature in 7 fractions à 500 µl of 0.1 N acetic acid and were analysed by 12% SDS-PAGE to evaluate yield and purity.

Purification and concentration of HLA-I peptides. Eluted HLA-I peptides and the subunits of the HLA complex were loaded on Sep-Pak tC18 (Waters) cartridges that were pre-washed with 80% acetonitryl (ACN) in 0.1% trifluoroacetic acid (TFA) and with 0.1% TFA only. After loading, the cartridges were washed with 0.1% TFA. The peptides were separated from the HLA-I heavy chains on the C18 cartridges, based on their hydrophobicity. The peptides were eluted with 30% ACN in 0.1% TFA. HLA-I peptides were further purified using Silica C-18 column (Harvard Apparatus, MA) tips and eluted again with 30% ACN in 0.1% TFA. The peptides were concentrated and the volume was reduced to 15 µl using vacuum centrifugation. For the mass spectrometry analysis 5 µ l of the highly enriched HLA peptides sample were used.

LC-MS/MS analysis of HLA peptides. HLA peptides were separated by a nanoflow HPLC (Proxeon Biosystems, now Thermo Fisher Scientific) and coupled on-line to a Q Exactive mass spectrometer (Thermo Fisher Scientific) with a nanoelectrospray ion source (Proxeon Biosystems). The column (20 cm long, 75 µm inner diameter) is packed in-house with

ReproSil-Pur C18-AQ 1.9 µm resin (Dr. Maisch GmbH, Ammerbuch-Entringen, Germany) in buffer A (0.5% acetic acid). Peptides were eluted with a linear gradient of 2–30% buffer B (80% ACN and 0.5% acetic acid) at a flow rate of 250 nl/min over 90 min. Data was acquired using a data-dependent 'top 10' in order to isolate them and fragment them by higher energy collisional dissociation (HCD). Full scan MS spectra were acquired at a resolution of 70,000 at 200 m/z with a target value of 3,000,000 ions. The ten most intense ions were sequentially isolated and accumulated to an AGC target value of 100,000 with a maximum injection time of 120 to increase signal of the fragments. Unassigned precursor ion charge states, as well as 4 and above charged species were rejected and peptide match was disabled. The fragmentation spectra of ions were acquired in the Orbitrap analyser with a resolution of 17,500 at 200 m/z.

Mass spectrometry data analysis of HLA peptides. MaxQuant computational proteomics platform (Cox and Mann, 2008) version 1.3.10.14 was used. Andromeda, a probabilistic search engine incorporated in the MaxQuant framework (Cox et al., 2011), was used to search the peak lists against the UniProt database (86,749 entries). N-terminal acetylation and methionine oxidation were set as variable modifications. The second peptide identification option in Andromeda was enabled. For statistical evaluation, the posterior error probability and false discovery rate were used. A false discovery rate of 0.01 was required for peptides and no false discovery rate was required for proteins, using a reverse database with no special AAs. The enzyme specificity was set as unspecific. A length restriction of 8 to 15 SS. was set, or a maximum peptides mass of maximum 1,500 Da. The initial mass deviation of the precursor ion was set up to 6 ppm and the fragment mass deviation was set up to 20 ppm. The 'match between runs' option was enabled, that allows matching of identifications across different replicates, in a time window of 0.5 min.

Supplementary Table

Table S1. List of 45 HLA-A02:01 epitopes from GPC3 protein that were predicted using three algorithms. The thresholds for a peptide being a binder in each of the tools were set to SYFPEITHI score ≥ 22 (29 sequences)[1], NetMHC predicted affinity ≤ 500 nM (27 sequences) [2,3] and BIMAS half time ≥ 20 min (27 sequences).[4] Fourteen peptides were predicted as binders by all three tools. Among them, marked in red, are the epitopes that were identified by our MS-based peptidomics analysis. NA indicates that the prediction score was below the threshold.

Position	Peptide	SYFPEITHI score	NetMHC: predicted affinity in nM	BIMAS Score: Estimate of t½ in min	Predicted by all three tools
10	L V V A M L L S L	23	234	NA	
14	M L L S L D F P G	NA	142	NA[	
44	R L Q P G L K W V	27	83	879.833	X
92	L L Q S A S M E L	24	27	36.316	X
102	F L I I Q N A A V	26	13	319.939	X
109	A V F Q E A F E I	NA	166	NA	
111	F Q E A F E I V V	NA	287	NA	
142	F E F V G E F F T	NA	NA	78.672	
144	F V G E F F T D V	NA	33	828.699	
149	F T D V S L Y I L	NA	131	NA	
153	S L Y I L G S D I	22	NA	33.385	
155	Y I L G S D I N V	24	11	162.769	X
162	N V D D M V N E L	22	NA	NA	
166	M V N E L F D S L	NA	230	NA	
169	E L F D S L F P V	23	3	1055.631	X
173	S L F P V I Y T Q	22	250	NA	
186	G L P D S A L D I	NA	NA	42.774	
197	C L R G A R R D L	22	NA	NA	
206	K V F G N F P K L	NA	161	45.992	
215	I M T Q V S K S L	NA	NA	26.228	
222	S L Q V T R I F L	22	432	117.493	X
229	F L Q A L N L G I	22	13	47.991	X
232	A L N L G I E V I	27	NA	NA	
254	R M L T R M W Y C	NA	157	1259.523	
281	V M Q G C M A G V	24	16	196.407	X
295	Y W R E Y I L S L	22	NA	NA	
299	Y I L S L E E L V	23	12	79.757	X
302	S L E E L V N G M	24	NA	NA	
315	D M E N V L L G L	22	NA	NA	
318	N V L L G L F S T	NA	NA	32.184	
319	V L L G L F S T I	26	40	124.682	X
326	T I H D S I Q Y V	23	50	**496.006**	X
340	K L T T T I G K L	26	NA	22.356	
367	F I D K K V L K V	**27**	**28**	40.472	X
383	T L S S R R R E L	22	NA	NA	

408	Y I C S H S P V A	NA	428	NA	
420	T L C W N G Q E L	22	NA	21.362	
451	K M K G P E P V V	22	NA	NA	
461	Q I I D K L K H I	23	NA	NA	
512	G M I K V K N Q L	22	NA	NA	
518	N Q L R F L A E L	NA	208	70.041	
522	F L A E L A Y D L	27	5	402.895	X
554	N L G N V H S P L	NA	NA	21.362	
564	L L T S M A I S V	23	17	118.238	X
571	S V V C F F F L V	NA	12	254.849	
Total number of predicted		**29**	**27**	**27**	**14**

Supplementary Literature

1. Rammensee H, Bachmann J, Emmerich NP, et al. SYFPEITHI: database for MHC ligands and peptide motifs. Immunogenetics 1999;50:213-9.
2. Nielsen M, Lundegaard C, Worning P, et al. Reliable prediction of T-cell epitopes using neural networks with novel sequence representations. Protein Sci 2003;12:1007-17.
3. Lundegaard C, Lamberth K, Harndahl M, et al. NetMHC-3.0: accurate web accessible predictions of human, mouse and monkey MHC class I affinities for peptides of length 8-11. Nucleic Acids Res 2008;36:W509-12.
4. Parker KC, Bednarek MA, Coligan JE. Scheme for ranking potential HLA-A2 binding peptides based on independent binding of individual peptide side-chains. J Immunol 1994;152:163-75.